


A Mathematical Model for Experimental Head-Flow Rate Curve of Partial Emission Pumps

Wenguang Li* 

School of Mathematics and Statistics, University of Glasgow, Glasgow, G12 8QQ, UK

ABSTRACT

The head-flow rate curve of the partial emission pump is flat and with a sudden drop-off near the maximum flow rate. Thus, it is difficult to fit the experimental head-flow rate curve of the pump by using a polynomial, which is suitable for centrifugal pumps. To tackle this problem, a new mathematical model was put forward in the inspiration of the mathematical model of the equivalent electric circuit of photovoltaic cells/modules. The physics behind the model was described by using flow rate saturation effect in partial emission pumps. The model was implemented in Excel and applied to the experimental head-flow rate data of seven partial emission pumps with different specific speeds in a range of 17-80. The model can produce high-quality curve fitting (coefficient of determination of greater than 0.9), The model is adaptive to the variable experimental head-flow rate data of partial emission pumps due to changes in impeller structure, rotational speed, number of blades and impeller diameter. Further, the model can fit the experimental head-flow rate data with drooping effect at low flow rate in partial emission pumps satisfactorily (coefficient of determination of greater than 0.94). The model potentially can be used in experimental data processing in the pump industry and pump-system modelling for partial emission pumps in future.

Keywords: Curve fitting; Flow rate; Head; Mathematical model; Partial emission pump

History

Received: 03.11.2023

Accepted: 25.02.2024

How to cite this paper:

Author Contacts

*Corresponding Author

e-mail addresses : wenguang.li@glasgow.ac.ukLi, W., (2024). A Mathematical Model for Experimental Head-Flow Rate Curve of Partial Emission Pumps. Engineering Perspective, 4(1), 1-6. <http://dx.doi.org/10.29228/eng.pers.74533>

1. Introduction

Partial emission pumps, as shown in Figure 1, are special centrifugal pumps developed in the 1960s, and have found extensive applications in aerospace, chemical, petroleum-chemical industries [1, 2], offshore technology [3] and so on. The pumps have an open impeller with straight radial blades in 90° blade discharge angle (measured from the reverse direction of the impeller rotation) [4].

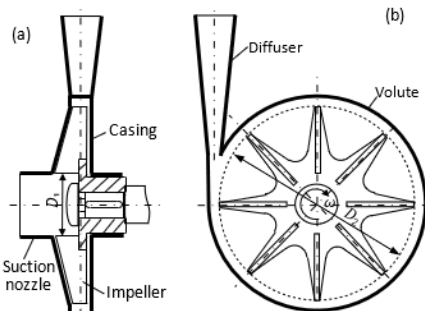


Figure 1. Impeller and volute configuration of a partial emission pump, (a) axial-cross-sectional view, (b) cross-sectional view in volute mid-span

dramatic sharp cut-off at the maximum flow rate in the experiment, as shown in Figure 2. Usually, a 2nd- or 3rd-order polynomial, which is mostly applicable to best fit the head-flow rate curve of centrifugal pump, is invalid for a partial emission pump. How to fit this kind of head-flow rate curve is concerned in the article.

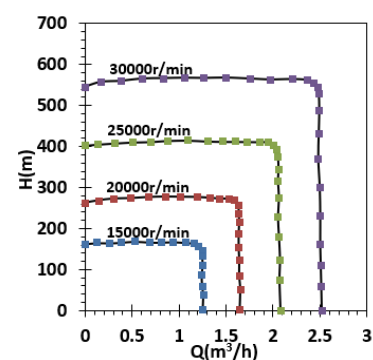


Figure 2. Experimental head-flow rate curves at the rotational speeds of 15000, 20000, 25000 and 30000r/min, the data are after [1]

As a result, the pumps often have a flat head-flow rate curve with

2. Model and method

2.1 Current-voltage model for photovoltaic cells or modules

The author had conducted a few modelling studies on the electric circuit of flat photovoltaic (PV) cells or modules [5-8]. A flat monocrystalline PV cell or module can be presented by using a single diode equivalent circuit with five combined parameters such as photocurrent, I_{ph} , diode reversal saturation current, I_d , diode quality factor, M , combined series resistance, R_s , and shunt resistance, R_{sh} [5], as shown in Figure 3a. The performance curve, i.e. I - V curve for the PV cell can be expressed mathematically by [5]:

$$I = I_{ph} - I_d \left[\exp \left\{ \frac{q(V + R_s I)}{MkT} \right\} - 1 \right] - \frac{V + R_s I}{R_{sh}} \quad (1)$$

where V and I are the output voltage and current of the PV cell/module, respectively; T is cell temperature, q is the electron charge, $q=1.60217646 \times 10^{-19}$ C, and k is the Boltzmann constant, $k=1.38065031 \times 10^{-23}$ J/K. I_{ph} depends on both solar radiation intensity and cell temperature in the silicon layer, while I_d is only cell-temperature dependent. A set of I - V data of a PV module was fitted by using Eq. (1), and good agreement between the data and the model is achieved, as shown in Figure 3b. This fact suggests that the exponential term in Eq. (1) can properly describe the rapid drop in the current when the voltage is beyond a certain value.

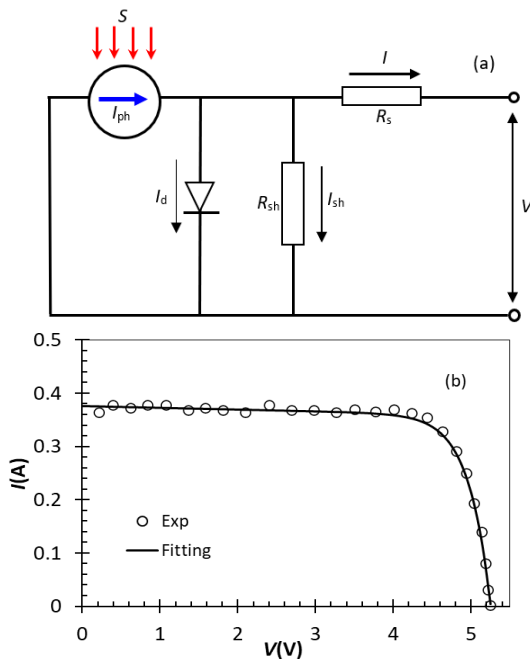


Figure 3. Single diode equivalent circuit of a flat monocrystalline PV module (a), and the experimental current-voltage (I - V) curve of the module at the standard solar radiation intensity $S=1000\text{W/m}^2$ (b), the plots are adopted from [5]

Physically, active electrons can be activated in a PV cell of semiconductor materials at a solar radiation intensity and cell temperature. The active electrons can travel to the p-side from the n-side in the cell to form a current inside the cell. If the cell is connected to a circuit, the active electrons will go back to the n-side to combine with the holes left by the electrons through the circuit outside the cell, thus

a current can be established in the circuit. The number of active electrons in the n-side generated per unit time is fixed at a given solar radiation intensity and cell temperature [9]. Therefore, the current curve exhibits a saturation property after the voltage is lower than a critical value as shown in Figure 3b. This saturation or choke behaviour is represented properly by the exponential function in Eq. (1).

2.2 Head-flow rate model for the pumps

The head-flow rate curves in Figure 2 are very similar to the current-voltage curve of the PV module in Figure 3b. Thus, an exponential function term should be involved in the mathematical model for head-flow rate curves of a partial emission pump. Inspired by the mathematical model of PV cells/modules, the following mathematical formula is proposed to fit the experimental data in Figure 2:

$$H = H_0 + aQ + bQ^2 - ce^{dQ^m} \quad (2)$$

where H and Q are pump head and flow rate, the coefficients $H_0(>0)$, a , b , $c(>0)$, $d(>0)$, and $m(>0)$ are determined based on a set of experimental H and Q data by using the least-squares method in Excel, and the number of scattered points of experimental data should be more than six. H_0 is the head at shut-off point. If $c=0$, then the 2nd-order polynomial for fitting head-flow rate curves of ordinary centrifugal pumps is recovered. The 2nd-order polynomial in Eq. (2) plays a role in fitting the flat part of a head-flow rate, but the exponential term takes the dramatic drop in the head-flow rate curve into account.

2.3 Method

The regression of Eq. (2) was performed against experimental data available by employing **Solver** in Excel. **Solver** is an add-in toolbox. It can be added into **Data** menu in Excel by clicking **File->Options->Add-ins->Solver**. The following steps are recommended to perform a slightly complicated curve fitting with a user mathematical model in Excel:

- 1) Experimental data of head and flow rate of a partial emission pump are read into Excel by occupying two columns;
- 2) Assign three columns to accommodate the initial and fitted coefficients, statistics results, head predicted with Eq. (2) and squared errors between the experimental head and the head predicted, respectively;
- 3) Calculate the sum of the squared errors and define it as the objective function by launching **Formula->Sum**;
- 4) Launch **Solver** to display the interface for the least-squares method by clicking **Data->Solver**, define the cell for reading and showing the objective function, optimization option, optimization algorithm;
- 5) **Run Solver**, if a converged solution has been resulted, check the coefficient of determination, R^2 , compare the experimental and predicted heads; if not, alter the initial values of the fitted coefficients until a satisfactory solution is achieved.

An example of setup for experimental head-flow rate data, predicted head, coefficients, statistical results, and the interface of **Solver** for coefficient optimization is illustrated in Figure 4. In the figure, cells H73-H78 are used to store the initial and optimized five

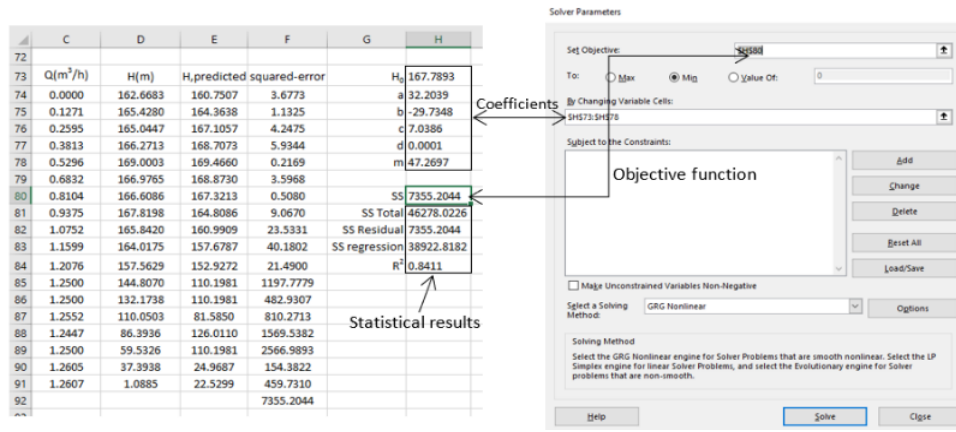


Figure 4. Experimental head-flow rate curve fitting set-up by using Solver in Excel, the right-experimental data, coefficients, model prediction, objective function, and statistical results, the left-interface of Solver for coefficient optimization, SS-sum of squares; in Excel cells, SS Total: H81=COUNT(D74:D91)*VARP(D74:D91), SS Residual: H82=SUMXMY2(D74:D91,E74:E91), SS Regression: H83=H81-H82, R²: H84=H83/H81, In Excel, COUNT is the function counts the number of cells that contain numbers; VARP is the function that calculates variance based on the entire population, SUMXMY2 is the function that returns the sum of squares of differences of corresponding values in two arrays, R² is the coefficient of determination, a statistical measure that uses the variance of one variable to explain the variance of another, R²=(SS Total-SS Residual)/SS Total

coefficients, cell H80 is for the sum of errors squared in head, cells H81-H84 accommodate the statistical results, cells E74-E91 are utilized to predict a head with six coefficients and a known flow rate, say cell E74 should be assigned with a formula such as $H_{74}+H_{74} * C_{74} + 1 * H_{75} * C_{74}^2 - H_{76} * \text{EXP}(H_{77} * C_{74} * H_{78})$ and so on, where cell C74 represents the flow rate. If the 2nd-order term is expected to exclude from Eq. (2), the '1' in the formula is altered to '0', i.e. $1 * H_{75} * C_{74}^2 > 0 * H_{75} * C_{74}^2$.

In the curve fitting process for **Solver**, a set of initial values of the coefficients H_0 , a , b , c , d , and m is needed. A few sets of initial values should be tried until **Solver** is convergent with a better coefficient of determination. Once the Solver is convergent with a satisfactory coefficient of determination, the coefficients H_0 , a , b , c , d , and m will be unique.

3. Results

Because the experimental data relating to partial emission pumps were very limited in the literature, firstly, the head-flow rate curve fitting model and method above were applied to five experimental partial emission pumps with very low specific speeds such as $n_s=23$ [1], $n_s=20$ [10], $n_s=19$ [11], $n_s=17$ [12], and $n_s=31$ [13]. The predicted heads are compared with the measurements in Figure 5. The determined corresponding coefficients in Eq. (2) are listed in Table 1 and 2. The specific speed of partial emission pumps is defined at best efficiency point or duty point by:

$$n_s = \frac{3.65n\sqrt{Q}}{H^{3/4}} \quad (3)$$

where n is pump rotative speed, r/min, H is pump head, m, Q is pump flow rate, m³/s. The experimental data in Figure 5a, 5d and 5e demonstrate the head-flow rate curves as the impeller rotational speed, number of blades and impeller diameter vary.

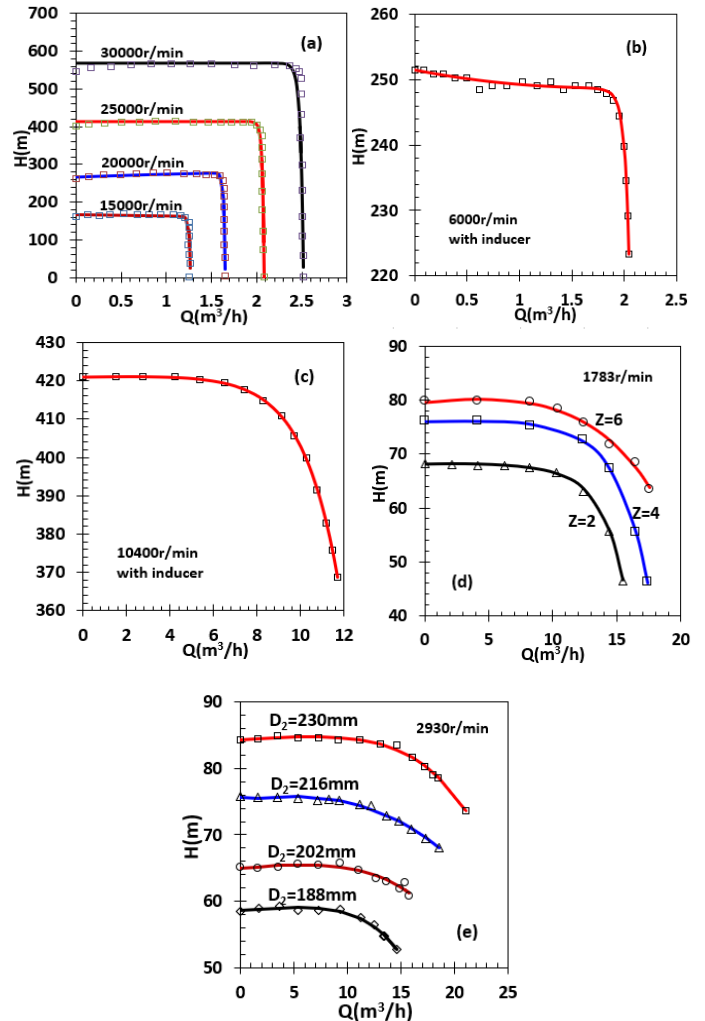


Figure 5. Experimental and fitted head-flow rate curves of existing four partial emission pumps found in the literature, (a) $n_s=23$ [1], (b) $n_s=20$ [10], (c) $n_s=19$ [11], (d) $n_s=17$ [12], (e) $n_s=31$ [13], the lines for fitted curves with Eq. (2), Z -number of blades, D_2 -impeller diameter, the symbols represent the experimental data in [1], [10]-[13], respectively

Table 1 Coefficients in Eq. (2) for the cases shown in Figure 5a-5c

Coef- ficient	$n(r/min)$					
	Figure 5a				Figure 5b	Figure 5c
	15000	20000	25000	30000	6000	10400
$H_0(m)$	178.2723	267.2406	413.2755	567.5908	251.4171	421.0318
a	-3.5770	9.2860	1.8542e-13	1.8542e-13	-3.1045	1.1534e-1
b	-29.7348	-1.5236	1.9029e-2	1.9231e-2	9.0563e-1	-3.0905e-3
c	11.2971	1.5490e-4	3.1838e-5	8.2953e-5	1.7311e-2	4.3175e-1
d	5.9866e-5	2.4978e-1	1.0476e-1	1.3744e-1	6.0485e-2	6.0946e-1
m	46.0748	8.0596	6.8938	5.1233	6.7033	1.0000
R^2	0.8380	0.8882	0.9091	0.8978	0.9954	0.9999

Table 2 Coefficients in Eq. (2) for the cases in Figure 5d and 5e

Coeffi- cient	Z in Figure 5d			$D_2(mm)$ in Figure 5e			
	2	4	6	230	216	202	188
$H_0(m)$	76.0433	79.6560	68.0717	84.4175	78.4502	64.9253	58.5929
a	0.0593	0.3438	0.0682	0.2026	0.8971	0.2248	0.1569
b	-0.0029	-0.0201	-0.0123	0	0	0	0
c	0.0418	0.0939	0.0246	0.1888	2.7750	0.0232	0.0174
d	0.3062	0.6112	0.1736	0.3128	0.3269	1.4085	0.9521
m	1.0734	0.7420	1.3341	0.8666	0.6648	0.5094	0.6960
R^2	0.9995	0.9926	0.9990	0.9934	0.9930	0.9171	0.9857

In Figure 5a, the curve fitting is slightly poor because the coefficients of determination are $R^2=0.84, 0.89, 0.91, 0.90$ at 15000, 20000, 25000, 30000r/min, respectively, in Table 1. R^2 is the coefficient of determination reflecting the proportion of the variation in head that is predictable from flow rate. In the other cases, as shown in Figure 5b-e, the curve fittings are quite good since the coefficients of determination are as great as $R^2=0.92-0.99$ shown in Table 2. These facts suggest that the mathematical model expressed by Eq. (2) is applicable to the cases with fixed impeller rotational speed and geometry but also is adaptive to the change in either impeller speed or geometry.

Secondly, the experimental data of additional two partial emission pumps with a bit high specific speeds at $n_s=69, 80$ in [2] were fitted by using Eq. (2) and are compared with the fitting curves in Figure 6, meanwhile the corresponding fitting coefficients are listed in Table 3. The variation of the experimental head against the flow rate is more complicated than that in Figure 5, the fitting is not perfect near the region where the head starts to drop off sharply. In other words, the fitting curves near that region are smoother than those in the experimental data. Consequently, the R^2 values are in the range of 0.94-0.98. Overall, the fitting results are satisfactory.

4. Discussion

As shown in Figure 5, the head curve of three partial emission pumps is flat in a wide range of flow rate and then drops off with increasing flow rate. One may think that the flat part in the head curve would be the most suitable for the operation of partial emission pumps and it is sufficient to fit the flat part in the curve rather than the whole curve. Unfortunately, the pump efficiency in the flat part

of the curve is lower than in the elbow of the curve, see Figure 7. To achieve a better efficiency, a partial emission pump can operate in the elbow of the curve. In this case, fitting the whole head curve of the pump is necessary.

The rapid drop in the head with increasing flow rate shown in Figure 2 is due to the saturation or choke effect of flow through the diffuser throat of the volute at a high flow rate. Also, this effect results in a large amount of hydraulic loss in the volute or even cavitation at the volute tongue [13] and leads to a remarked head drop. Obviously, this effect resembles the current saturation or choke behaviour in a PV cell. The exponential function of the last term in Eq. (2) is employed to handle this effect mathematically.

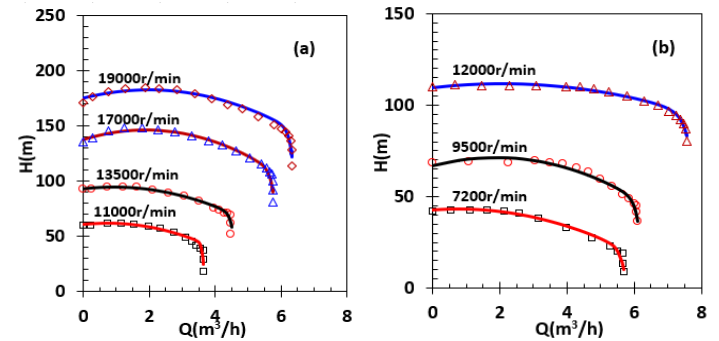
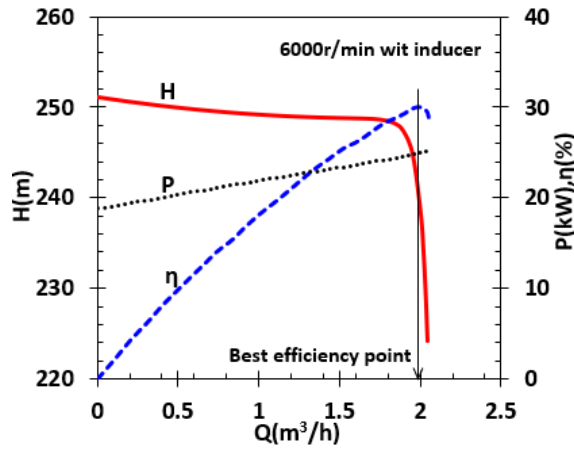


Figure 6. Experimental and fitted head-flow rate curves of existing two partial emission pumps found in [2], (a) $n_s=69$, (b) $n_s=80$, the lines for fitted curves with Eq. (2), the symbols represent the experimental data in [2]

Table 3 Coefficients in Eq. (2) for the cases shown in Figure 6

Coefficient	$n(\text{r/min})$						
	Figure 6a			Figure 6b			
	11000	13000	17000	19000	7200	9500	12000
$H_0(\text{m})$	60.5195	92.9577	137.9416	175.0071	42.4756	67.0659	109.5380
a	3.1587	3.4674	9.2794	7.4943	1.3438	4.7721	2.1250
b	-2.1351	-1.8603	-2.4424	-1.8765	-8.8415e-1	-1.2698	-5.1330e-1
c	1.9932e-5	1.5943e-3	4.5343e-4	2.1998e-5	1.6318e-5	2.9735e-4	1.4335e-3
d	4.2687e-3	7.3030e-4	1.0976e-3	3.2434e-3	4.5655e-2	1.4251e-3	2.1222e-3
m	6.2347	6.2700	5.2426	4.5320	3.2659	4.9244	4.1350
R^2	0.9459	0.9536	0.9467	0.9623	0.9779	0.9768	0.9866

Figure 7. Head H , shaft-power P and efficiency η curves of the partial emission pumps tested in [10].

In pump industry and its application sectors, the head-flow rate curve of centrifugal pumps is usually expressed by using a 2nd or even higher order polynomial, for example, in the work presented in [14-18]. Furthermore, orthogonal polynomials are employed to fit experimental data of centrifugal or axial-flow pumps [19]. Interestingly, the following mathematical model was proposed to fit the experimental data of head of centrifugal pumps [20]:

$$H = H_0 - ce^{dq} \quad (4)$$

where H_0 , c and d are fitting coefficients. Obviously, Eq. (4) is a simplified version of Eq. (2) when the conditions: $a=b=0$ and $m=1$ are held. Therefore, the work presented in the paper is innovative to partial emission pumps.

In Figure 5c-5e, the head reduces more gently with increasing flow rate than in Figure 5a and 5b, and the head-flow rates resemble to the curves of centrifugal pumps, thus the m values are close to 1, as shown in Table 1 and 2. Hence, the mathematical model Eq. (2) are suitable for centrifugal pumps as well.

5. Conclusions

A mathematical model was proposed for the experimental head-flow rate curve fitting of partial emission pumps and implemented in Excel. The physics behind the model was explained based on the flow rate saturation effect in the pumps. The model can produce high-quality curve fitting based on the experimental head-flow rate data of seven partial emission pumps collected in the literature and is more general than the existing mathematical models. It is hopeful

that the model can find applications to experimental data processing in the pump industry soon. The author can provide the supplementary data in Excel file on request.

Acknowledgment

This study was not supported by a project, thus no funding source was appreciated.

Nomenclature

a	coefficient in Eq. (2)
b	coefficient in Eq. (2)
c	coefficient in Eq. (2)
d	coefficient in Eq. (2)
D_1	inlet diameter of impeller (mm)
D_2	outlet diameter of impeller (mm)
H	pump head (m)
H_0	coefficient in eq. (2) (m)
I	output current of flat photovoltaic cell/module (A)
I_d	diode reversal saturation current shown in Figure 3a (A)
I_{ph}	photocurrent shown in Figure 3a (A)
k	Boltzmann constant, $k=1.38065031 \times 10^{-23} \text{J/K}$
n	rotational speed of impeller (r/min)
m	power in Eq. (2)
M	diode quality factor
n_s	pump specific speed defined by Eq. (3)
q	electron charge, $q=1.60217646 \times 10^{-19} \text{C}$
P	pump shaft-power (kW)
Q	pump flow rate, (m^3/h) or (m^3/s)
R_s	combined series resistance shown in Figure 3a (Ω)
R_{sh}	shunt resistance shown in Figure 3a (Ω)
R^2	coefficient of determination defined in caption of Figure 4
S	solar radiation intensity (W/m^2)
T	cell temperature (K)
V	Output voltage of flat photovoltaic cell/module (V)
Z	number of blades
η	pump efficiency (%)

ω	rotational angular speed of impeller (rad/s)
PV	photovoltaic
SS	sum of squares

Conflict of Interest Statement

The author declares that there is no conflict of interest in the study.

CRediT Author Statement

Wenguang Li: Conceptualization, Methodology, Software, Writing-original draft, review, and editing.

References

1. Barske, U. M. (1960). Development of some unconventional centrifugal pumps. *Proceedings of Institute of Mechanical Engineers*, 174, 437-461.
2. Lock, T. (1966). A forced vortex pump for high speed, high pressure, low flow applications. *SAE Transactions*, 74, 729-737.
3. Finder, P. (2022). Partial Emissions Pump Series' Dual PEP. Accessed December 24, 2022. Available at <https://www.offshore-technology.com/contractors/pumps/finder-pompe/pressreleases/dual-pep-series/>
4. Li, W. (2021). Affinity laws for impellers trimmed in two partial emission pumps with very low specific speed. *Proc IMechE Part C: Journal Mechanical Engineering Science*, 235, 859-877.
5. Li, W., Paul, M. C., Sellami, N. et al. (2016). Six-parameter electrical model for photovoltaic cell/module with compound parabolic concentrator. *Solar Energy*, 137, 551-563.
6. Li, W., Paul, M. C., Rolley, M. et al. (2017). A coupled optical-thermal-electrical model to predict the performance of hybrid PV/T-CCPC roof-top systems. *Renewable Energy*, 112, 166-186.
7. Li, W., Paul, M. C., Rolley, M. et al. (2017). A scaling law for monocrystalline PV/T modules with CCPC and comparison with triple junction PV cells. *Applied Energy*, 202, 755-771.
8. Li, W., Paul, M. C., Baig, H. et al. (2019). A three-point-based electrical model and its application in a photovoltaic thermal hybrid roof-top system with crossed compound parabolic concentrator. *Renewable Energy*, 130, 400-415.
9. Hersch, P. & Zweibel, K. (1982). *Basic Photovoltaic Principles and Methods*, SERI/SP-290-1448, Oak Ridge: Technical Information Office.
10. Wilk, A. (2008). Pressure distribution around pump impeller with radial blades: Proceedings of 6th IASME/WSEAS International Conference on Fluid Mechanics and Aerodynamics, Rhodes, Greece, August 20-22.
11. Shui, Q., Jiang, T., Pan, B. et al. (2021). Numerical research on performance of high-speed partial emission pump. *Shock and Vibration*, Article ID 6697063.
12. Turton, R. K. (1973). *The open impeller pump*, Process Pumps. Institution of Mechanical Engineers: London, UK.
13. Fan, Z. L., & Wang, G. T. (2002). Experiment on partial emission pumps. *Pump Technology*, 2, 3-8.
14. Yang, Z. & Børsting, H. (2010). Energy efficient control of a boosting system with multiple variable-speed pumps in parallel: Proceedings of the 49th IEEE Conference on Decision and Control Hilton Atlanta Hotel, Atlanta, USA, December 15-17.
15. Chang, W., Chang, J. W., Yin, H. et al. (2012). Energy-saving algorithm for pumping systems based on fuzzy decision making: Proceedings of the IEEE International Conference on Systems, Man, and Cybernetics, COEX, Seoul, Korea, October 14-17.
16. Luo, Y., Yuan, S., Sun, H. et al. (2015). Energy-saving control model of inverter for centrifugal pump systems. *Advances in Mechanical Engineering*, 7, 1-12.
17. Cheng, Q., Ma, Y., Yang, J. et al. (2019). Fitting and correction of H-Q performance curve of centrifugal pump. *Journal of Petrochemical Universities*, 32, 78-84.
18. Müller, T. M., Leise, P., Lorenz, I. et al. (2021). Optimization and validation of pumping system design and operation for water supply in high-rise buildings. *Optimization and Engineering*, 22, 643-686.
19. Zhou, L. C. & Qiu, C. X. (2001). Orthogonal polynomial fitting for pump characteristic curves. *Drainage and Irrigation Machinery*, 19, 8-11.
20. Liao, L., Lin, J., Zhang, C. (2002). Efficiency optimization of variable frequency variable speed water-supply pumping stations based on genetic algorithm. *Engineering Science*, 4, 54-58.